HHS Public Access

Author manuscript

Acta Biomater. Author manuscript; available in PMC 2015 April 15.

Published in final edited form as:

Acta Biomater. 2012 December ; 8(12): 4268–4277. doi:10.1016/j.actbio.2012.08.002.

Microstructural manipulation of electrospun scaffolds for specific bending stiffness for heart valve tissue engineering☆

Nicholas J. Amoroso[a,b], **Antonio D'Amore**[a,b,e,f], **Yi Hong**[b], **Christian P. Rivera**[b], **Michael S. Sacks**[a,1], and **William R. Wagner**[a,b,c,d,*]

[a] Department of Bioengineering, University of Pittsburgh, Pittsburgh, PA 15219, USA

[b] McGowan Institute for Regenerative Medicine, University of Pittsburgh, Pittsburgh, PA 15219, USA

[c] Department of Chemical Engineering, University of Pittsburgh, Pittsburgh, PA 15219, USA

[d] Department of Surgery, University of Pittsburgh, Pittsburgh, PA 15219, USA

[e]*Foundation RiMED, Palermo 90133, Italy*

[f]*DICGIM, University of Palermo, Italy*

Abstract

Biodegradable thermoplastic elastomers are attractive for application in cardiovascular tissue construct development due to their amenability to a wide range of physical property tuning. For heart valve leaflets, while low flexural stiffness is a key design feature, control of this parameter has been largely neglected in the scaffold literature where electrospinning is being utilized. This study evaluated the effect of processing variables and secondary fiber populations on the microstructure, tensile and bending mechanics of electrospun biodegradable polyurethane scaffolds for heart valve tissue engineering. Scaffolds were fabricated from poly(ester urethane) urea (PEUU) and the deposition mandrel was translated at varying rates in order to modify fiber intersection density. Scaffolds were also fabricated in conjunction with secondary fiber populations designed either for mechanical reinforcement or to be selectively removed following fabrication. It was determined that increasing fiber intersection densities within PEUU scaffolds was associated with lower bending moduli. Further, constructs fabricated with stiff secondary fiber populations had higher bending moduli whereas constructs with secondary fiber populations which were selectively removed had noticeably lower bending moduli. Insights gained from this

---

☆Part of the Special Issue "Advanced Functional Polymers in Medicine (AFPM)", guest editors: Professors Luigi Ambrosio, Dirk W. Grijpma and Andreas Lendlein.

*Corresponding author at: McGowan Institute for Regenerative Medicine, University of Pittsburgh, Pittsburgh, PA 15219, USA. Tel.: +1 412 235 5146; fax: +1 412 235 5160. wagnerwr@upmc.edu (W.R. Wagner)..

[1]Present address: Department of Biomedical Engineering and The Institute for Computational Engineering and Sciences, University of Texas at Austin, Austin, TX, USA.

Appendix A. Figures with essential colour discrimination

Certain figures in this article, particularly Figs. 1–9, are difficult to interpret in black and white. The full colour images can be found in the on-line version, at http://dx.doi.org/10.1016/j.actbio.2012.08.002.

Appendix B. Supplementary data

Supplementary data associated with this article can be found, in the online version, at http://dx.doi.org/10.1016/j.actbio.2012.08.002.

work will be directly applicable to the fabrication of soft tissue constructs, specifically in the development of cardiac valve tissue constructs.

Keywords

Electrospinning; Bending modulus; Mechanical characterization; Structural analysis; Heart valve tissue engineering

1. Introduction

Flexural rigidity is a functional measure that quantifies a key aspect of a surgeon's perception regarding the appropriateness of a biomaterial for soft tissue repair. Beyond meeting perceived mechanical requirements prior to material implantation, the selection of a material with appropriate flexural rigidity is functionally important in avoiding a mechanical mismatch in situ, which could lead to patient discomfort, tissue damage and a disruption of the desired healing process [1]. In the specific case of heart valve tissue engineering, flexural properties are of paramount importance to achieving appropriate valve function [2–4]. Specifically, however, scaffold flexural behavior is discussed least in the literature of the common mechanical responses.

The most common materials under development for the tissue engineering of heart valves include decellularized extracellular matrix (ECM)-based scaffolds [5,6] and synthetic fibrous scaffolds [7–9]. Decellularized ECM scaffolds are typically sourced from human or xenograft valvular tissue [10–12] or small intestinal submucosa [13,14]. However, decellularized, ECM-based scaffolds, depending upon the processing method employed, can be hindered by inconsistent performance in terms of their mechanics and local cytotoxicity due to residual processing agents [15].

Synthetic scaffolds have the advantage of consistent processing methodologies which can produce reliable and tunable mechanical properties and functional results. Varieties of non-woven fibrous scaffolds are commercially available and are typically based on polymers utilized in other devices that have obtained regulatory approval. Synthetic scaffolds can be seeded with cells [7–9] and have been shown to support host cell infiltration [16]. However, many of the current materials used to produce such scaffolds have been limited by their high stiffness and lack of mechanical anisotropy, and thus fail to approximate native valvular tissue [17].

One method of producing non-woven fibrous scaffolds is electrospinning, which is notable for the ability to generate structural features on the nano- to microscale [18]. Electrospun constructs are amenable to modification during, as well as following, fabrication to introduce functionality or modify microstructure and mechanical response. With respect to the latter, functional groups and peptides can be introduced onto electrospun fibers through common surface treatments [19] or by grafting them onto the polymer chain prior to solvent processing. Scaffold porosity and packing density can be altered by the introduction of a porogen such as salt crystals to create macropores [20], laser ablation of scaffolds following fabrication [21], or concurrently electrospraying an aqueous medium to loosen interactions

between polymer layers [16]. It is further possible to alter electrospun scaffold microstructure in order to create anisotropy within the constructs. Fibers can be patterned [22] or aligned [17] to encourage contact guidance of seeded cells [19] and produce tunable tensile mechanical anisotropy [17]. While such structural manipulations have been employed to alter the mechanical behavior of electrospun scaffolds under tension, a reliable method of controlling the inherent bending modulus would be desirable to provide a more complete approach to meeting design objectives for soft tissue constructs.

The objective of this study was to examine specific microstructural features important to determining the flexural behavior of electrospun scaffolds suitable for heart valve tissue engineering. Methods are highlighted for tuning the flexural response by modifying fabrication parameters, or by introducing secondary fiber populations that may have a higher modulus or be selectively dissolved from the scaffold following fabrication. The effect of such construct modifications on in-plane tensile properties is also demonstrated, and effort was made to mimic the mechanical properties of a native pulmonary valve in both flexural and equi-biaxial tensile response.

2. Materials and methods

2.1. Scaffold fabrication

Poly(ester urethane) urea (PEUU) was synthesized as described previously [23] from polycaprolactone diol (M_n = 2000, Sigma), 1,4-diisocyanatobutane (Sigma) and putrescine (Sigma). Scaffolds were fabricated in a manner similar to that previously reported [24]. Briefly, PEUU was dissolved in 1,1,1,3,3,3-hexafluoroisopropanol (HFIP) at a concentration of 12% (w/v) and electrospun onto a rotating and translating stainless steel mandrel (6 mm diameter) by feeding through a charged capillary (1.19 mm ID) at 1.5 ml h^{-1}. The mandrel was located 17 cm from the tip of the capillary and grounded with a voltage of −5 kV. The polymer feeding tube was charged to 12 kV. The mandrel was rotated with a tangential speed of 8 cm s^{-1} and translated along its axis at 0.3, 1.5, 3.0 or 30.0 cm s^{-1} (Fig. 1a).

Scaffolds were electrospun from PEUU in HFIP alone, or concurrently with a secondary polymer stream being fed from a capillary mounted in a separate location. Polycaprolactone (PCL, Sigma, M_n = 80,000 kDa) dissolved in HFIP (8% w/v) was electro-spun from a capillary in a 180° opposing orientation from PEUU, at volume flow ratios of 100:0, 75:25, 50:50, 25:75 and 0:100 PEUU:PCL. In separate experiments, poly(ethylene) oxide (PEO) (M_v = 200 kDa) in cell culture medium (Dulbecco's modified Eagle medium, 10% fetal bovine serum, 5% penicillin/streptomycin) was electrospun from a perpendicular orientation to PEUU in volume flow ratios of 100:0, 85:15, 75:25 and 50:50 PEUU:PEO. Following fabrication, PEO-incorporated scaffolds were placed in distilled water for at least 4 h, changing the water once, in order to dissolve the PEO fibers and to leach PEO out of the scaffold matrix. Scaffolds made from 25:75 PEUU:PEO did not maintain structural integrity following PEO fiber removal, and were therefore not included in the study. All mechanical characterizations of PEUU:PEO blended constructs were completed following dissolution of the sacrificial fibers. All experimental groups were fabricated with a minimum sample number of n = 5 independently processed scaffolds.

2.2. Imaging and structural analysis

Scaffold microstructure for all constructs was determined through scanning electron microscopy (SEM, JEOL JSM6330F) after gold sputter coating. The resultant images were analyzed using an automated algorithm to provide quantitative comparisons of the following microstructural features: fiber diameter, orientation index (alignment angle distribution) [25–27] and intersection density [28]. This algorithm is designed to limit analysis to the surface fibers of the scaffold in order to minimize the recognition of fiber intersections when two fibers are not in contact [28]. Fiber intersection density was normalized to fiber diameter for comparisons as previously presented [24]. The distribution and morphology of distinct fiber populations in multi-polymer constructs were visualized by adding fluorescein isothiocyanate isomer I (0.001%, Fluka BioChemika) to the PEUU solution prior to electrospinning and Rhodamine 101 (0.001%, Fluka BioChemika) to the PEO or PCL solution prior to electrospinning thin mats of only several fiber layers thick. These constructs were imaged under fluorescent microscopy (Olympus 1X71).

2.3. Mechanical testing

2.3.1. Uniaxial mechanical testing—Constructs previously immersed in distilled water were sectioned for uniaxial mechanical testing using a dog-bone-shaped punch (Ray-Ran Testing Equipment) and tested with an MTS Tytron 250 MicroForce Testing Workstation at a 25 mm min^{-1} cross-head speed according to ASTM D638-98. Mechanical testing of PEUU/PEO blended scaffolds was performed following PEO dissolution. Sections were cut from each specimen so that the long axis being tested was consistent with the longitudinal axis of the mandrel.

2.3.2. Suture retention strength—Suture retention testing was performed according to American National Standard Institute – Association for the Advancement of Medical Instruments (ANSI/AAMI) VP20 standards. Briefly, 5 mm × 15 mm strips of each scaffold were sectioned so that the long axis matched with the longitudinal axis of the mandrel. A single loop of 4-0 braided polyester suture (Syneture) was placed in each section with a 2 mm bite. The suture was then pulled at 120 mm min^{-1} using the same MTS Tytron 250 MicroForce Testing Workstation as above. Suture retention strength was defined as the peak load before pullout/(suture diameter sample × thickness).

2.3.3. Biaxial mechanical testing—For biaxial mechanical testing, 10 × 10 mm sections were removed from each construct type. Polypropylene suture (Ethicon) was cut to form four small markers of ~1 mm diameter which were affixed to form a square in the central region of each specimen. Samples were then floated in a room temperature physiological saline bath and subjected to a Lagrangian membrane tension (T) controlled protocol as previously described [24]. Equibiaxial tension was applied up to a maximum of 90 N m^{-1} to facilitate comparison with previous studies on valvular tissues [17,29]. Data post-processing was completed using a preconditioned free-float reference, and was converted to stresses using measured specimen dimensions.

2.3.4. Flexural mechanical testing—Flexural mechanical testing was performed as previously described [30]. Briefly, sections measuring 12 × 3 mm were removed from each

electrospun construct and reserved for flexural testing. Sections were dried and six markers were affixed at even spacing along the edge of each specimen. Samples were immersed in a room temperature saline bath and mounted in a custom made-holder (Fig. 1b). The holder and bath were then raised and lowered with respect to a vertical loading bar which measured bending moment (M) up to a maximum sample curvature of $\Delta\kappa = 0.15 – 0.25\ mm^{-1}$, comparable to the maximum curvature experienced by functioning pericardial bioprosthetic heart valve leaflets and reported in previous work involving valvular biomaterials [31]. Specimen dimensions were recorded automatically through imaging software, and used to calculate the second moment of area (I). The effective bending modulus (E) was calculated using the Bernoulli–Euler moment–curvature equation:

$$M = EI\Delta\kappa.$$

2.3.5. Statistical analyses—Statistical significance was determined using one way analysis of variance with the Holm–Sidak method for post hoc pairwise comparisons. Correlation coefficients were determined using Pearson's product moment correlation.

3. Results

3.1. Effect of mandrel translation on dry ePEUU

Altering the translational speed of the reciprocating target mandrel during electrospinning produced consistent microstructural and functional changes. These changes were subtle and not readily discernible by visual inspection of micrographs (Fig. 2a). Structural analysis uncovered a trend relating increased mandrel translational speed during fabrication to a decrease in fiber intersection density of the electrospun scaffolds without change in any other structural measure evaluated (Fig. 2b and c). Fiber diameters were not found to be significantly different between groups (data not shown). High resolution inspection of these fiber intersections demonstrated that fibers appear to be partially melded together at their interface (Fig. 2d). Under further evaluation, fiber intersection density was found to be strongly inversely correlated ($R = -1.00$, $p < 0.001$) with a decrease in flexural modulus (Fig. 3a). No statistically significant differences were observed in initial uniaxial tensile moduli or suture retention strength for these constructs (Fig. 3b and c). Further, no significant differences were observed in the ultimate tensile strength or elongation at failure between the constructs generated at different translational speeds (data not shown).

3.2. Effect of secondary fiber populations

Secondary fiber populations were introduced during construct fabrication to form uniform mixed fiber constructs of varying polymer ratios. Fluorescent dyes mixed with each polymer solution enabled visualization of independent fiber populations under confocal microscopy. Each fiber population appeared randomly distributed throughout each scaffold, and volume fractions of each polymer qualitatively matched that of the feed ratio used during fabrication (Fig. 4a). SEM micrographs qualitatively depict a greater range of fiber diameters present within the constructs; however, the fiber types cannot be differentiated under this imaging modality (Fig. 4b). Structural analysis demonstrated that intersection density tended to increase with higher quantities of PCL (Fig. 4c).

Adding an increasing volume fraction of PCL fibers within the construct increased the tensile modulus under uniaxial load (Fig. 5a). Under equal biaxial tension, all constructs containing PCL fibers were observed to be significantly ($p < 0.001$) more stiff and isotropic than unmodified PEUU fabricated under similar conditions (Fig. 5b). No additional stiffening was observed under biaxial tension at PCL concentrations above 25%. The addition of PCL fibers into PEUU scaffolds produced a significant increase in bending modulus. Fractional changes in the PEUU:PCL flow rate ratio resulted in changes to the observed bending moduli, with constructs containing the most PCL being more rigid in bending, while those with more PEUU remaining less stiff. The inclusion of any quantity of PCL fibers studied resulted in a significantly higher bending modulus than for simple PEUU scaffolds (Fig. 6).

Concurrent PEO and PEUU electrospinning produced constructs with fiber populations that appeared to be distinguishable by their diameters. Upon contact with water, constructs containing 75 and 50% PEO macroscopically contracted and curled slightly. No macroscopic changes were readily observed with constructs originally containing 15% PEO following water contact. The putatively smaller PEO fibers dissolved immediately upon contact with water, leaving PEUU fibers intact, but causing a distinct microstructural change. No changes in fiber morphology were appreciated following longer periods of water contact (Fig. 7a and b). Fiber intersection density within constructs that initially contained PEO fibers was higher following PEO dissolution than that found in similarly fabricated PEUU scaffolds without PEO fibers.

Qualitative assessment of scaffolds with dissolved PEO fiber populations found that these materials were more malleable than those made from PEUU alone. Constructs that initially contained 75% PEO did not maintain mechanical integrity following immersion in water, and were not further evaluated. Higher volume fractions of sacrificial fibers within the PEUU based scaffolds were associated with decreasing uniaxial tensile moduli ($p < 0.05$) following fiber removal (Fig. 8a). A selection of representative stress–strain curves for these multi-component scaffolds can be found in Supplemental materials Fig. S1. However, this did not appear to alter the suture retention strength of these constructs (Fig. 8b). Additionally, no significant difference was observed between any PEO blended scaffold and pure electrospun PEUU under equal biaxial tension (Fig. 8c). Scaffolds containing increasing initial amounts of PEO had a diminishing capacity to support their own weight when suspended as a cantilever following immersion in water compared with unmodified electrospun PEUU (Fig. 9a, Video 1, Supplemental materials). This general phenomenon was shown quantitatively by the relationship between increasing quantities of sacrificial fibers and progressively lower flexural moduli following submersion in water ($p < 0.05$, Fig. 9b). Scaffolds containing 50% PEO had a flexural modulus statistically higher than that of the native pulmonary valve, but which was of the same order of magnitude.

4. Discussion

How a biomaterial scaffold responds to physiologic loading is of critical importance to any tissue engineering application, and is of particular importance when seeking to reproduce the function of a cardiac valve. Materials utilized for valvular replacement will be subjected to

cyclic forces up to 400–600 kPa thousands of times per day, every day. For a biomimetic valvular replacement to function successfully, it must not succumb to mechanical fatigue and be capable of passively stretching in the radial direction, while also remaining unyielding in the circumferential direction under such forces [29]. Further, for natural leaflet movement, valvular materials must flex easily during normal function [4].

It is well established that electrospinning can be used to produce fibrous scaffolds with high levels of structural and mechanical anisotropy. During fabrication, fibers can be aligned through electrostatic or physical manipulation including high mandrel tangential velocities [32–35]. It has been shown that when such scaffolds comprise compliant elastomers, the biaxial mechanical response can be designed to closely mimic that found in the native heart valve leaflet under physiologic loads [17]. A prior report [24] has demonstrated that changes in the density of fiber intersections can be brought on without altering fiber orientation by introducing and varying the translational velocity of the collecting mandrel during fabrication. In this manner, fiber orientation index and intersection density could be decoupled, with orientation being controlled by mandrel rotation and intersection density by mandrel translation. This was possibly enabled by slow motion of the mandrel surface both in rotation and in translation, which could permit rapidly whipping fibers to deposit on top of one another more closely. A faster translational speed might create a more open structure. These subtle structural changes were also associated with changes in mechanical response. Low translational velocities were associated with higher fiber intersection densities, which were further associated with high strain energy and pronounced mechanical anisotropy under equal biaxial loads. However, to date reports seeking to understand the relationship between electro-spun scaffold morphology and flexural properties have been lacking.

In the present work, the major experimental finding was a strong inverse correlation between fiber intersection density and bending modulus within electrospun polyurethanes. This suggests a functional relationship between network intersection density and flexural mechanical response. This phenomenon presents an apparent contradiction, as higher cross-link densities would generally be thought to result in stiffer mechanical behavior. It is also noted that polymer mass fractions within constructs at different translational speeds were previously explored [24], and no significant differences were found. In speculating as to what might cause this effect, it is noted that the whipping and pulling motion of the electrospinning process introduces crystallinity into the individual polymeric fibers [17,36,37]. High magnification micrographs of fiber intersections demonstrate that fibers undergo some degree of melding at each intersection (Fig. 2d). These interaction points might serve to locally disrupt the crystalline structure within the respective fibers. If this were the case, a local amorphous region might function as a hinge point that facilitates bending on a micro-scale. The additive combination of these weak points could translate into a lower bulk bending modulus. Such a hypothesis remains to be explored. It may be possible to examine the local crystallinity at fiber intersections using selected area electron diffraction or a similar technique.

The potential to tune scaffold bending modulus was expanded upon by exploring the introduction of secondary fiber populations. PCL fibers were included within the PEUU fiber matrix as a means of mechanical reinforcement. Adding increasing volume fractions of

PCL fibers was found to increase tensile modulus under uniaxial tensile load. This was in approximate agreement with the rule of mixtures for non-unidirectional fiber reinforcement [38]. However, no tunable response in stiffness was observed under equi-biaxial tension, as even a small quantity of PCL produced constructs with markedly reduced compliance. One possible explanation for such disparity between uniaxial and biaxial responses is that PCL fibers were able to rotate during uniaxial loading, whereas this deformation was restricted under planar biaxial loading. Structurally, such scaffolds were found to possess larger densities of fiber intersections with increased PCL. This may be due to the secondary fiber source producing fibers independently from the PEUU fiber source. A larger quantity of deposited fibers in a given area would logically increase the density of intersections within a construct. As expected, increased quantities of the much stiffer PCL produced scaffolds with larger bending moduli. Through this method, it was possible to produce constructs with bending moduli comparable to more rigid tissues such as costal cartilage and intact septal cartilage [39,40].

A previous report by Baker et al. [41] introduced the technique of co-electrospinning PEO as a sacrificial fiber population in order to improve porosity and cell infiltration. Consistent with the results presented there, PEUU/PEO blended constructs possessed lower tensile moduli following removal of PEO fibers with increasing quantities of sacrificial PEO fibers. However, in the present work, a more dramatic microstructural change was observed following PEO dissolution. This difference is likely due to residual stress supported by the stiff PEO fibers as the construct was fabricated and is consistent with the work presented by Lowrey et al. [36]. Once those fibers were removed, the PEUU fibers were able to recoil. This may help explain the decrease in tensile modulus observed under uniaxial loading, as well as the further decrease in bending modulus. In this work, PEO was dissolved in cell culture media in order to facilitate comparison with previous studies [16]. This technique would also be amenable to encapsulating cells within the PEO fiber stream if the cells were not to be directly electrosprayed [42]. It is expected that some residual protein or PEO may adsorb onto the PEUU fibers. This would likely be in a mono-layer, and SEM images do not suggest cross-linked protein residue that might produce substantial mechanical effect. However, it was unexpected that introducing PEO fibers to the fabrication process appeared to produce constructs with higher fiber intersection densities than single stream PEUU scaffolds fabricated under similar conditions. Electrostatic interactions between the two positively charged fiber streams during fabrication may have had an effect on fiber deposition patterns.

The combination of low mandrel translational speed and the introduction of a sacrificial fiber population during fabrication was able to produce scaffolds with little resistance to bending. For soft tissue repair, in general, this is an attractive feature in scaffold development to prevent injury to healthy surrounding tissue as well as to ingrowing tissue during healing. For example, an ideal mesh for abdominal wall repair must also drape properly for optimal healing and surgical handling during implantation [1]. This behavior is directly related to the flexural rigidity of the mesh. The overall functional measure of flexural rigidity, neglecting tension and compression, is defined as $D = EI$, where I is the second moment of inertia, which is proportional to the thickness cubed. Therefore, it is

possible to decrease the thickness of any material in order to produce a tissue construct that is functionally less stiff in bending despite its modulus. However, this will necessarily be accompanied with decreased suture retention strength, increasing the risk of rupture at the anastomosis. Further, for degradable materials, there exists a minimal thickness necessary for appropriate tissue ingrowth and remodeling prior to mechanical failure. This would depend on the structure of the material, mechanical response and degradation rate in vivo. Constructs fabricated thinner than the critical thickness would be expected to prematurely degrade before ingrown tissue could mechanically function under physiologic loads in situ. Altering the bending modulus of a construct can allow for a greater range of flexural rigidity while maintaining adequate suture retention strength and preventing premature degradation.

Results presented in this paper demonstrate the capability of fabricating elastomeric scaffolds with good tensile strength, mechanical anisotropy, as well as a bending modulus that is significantly higher, but still on the order of magnitude of the native porcine pulmonary valve. By slightly decreasing the thickness of the construct (in the case of PEUU/PEO 50/50, by 13%), the methods described in this paper can be put into practice to produce mechanically strong elastomeric constructs with flexural rigidity equal to that of native heart valve tissue.

4.1. Limitations and future work

Several additional experiments logically follow this work in order to address the inherent limitations of the current study. No degradation or fatigue studies were performed in order to evaluate potential long term function of these constructs. However, it would be expected that without cells, as the material degrades, the material will necessarily weaken and fail. The tissue engineering paradigm would require cells to elaborate ECM to take over the mechanical load from the degrading polymer fibers. Therefore, investigation of long term function must be completed either in a mechanically controlled bioreactor or in vivo. Such a study would also evaluate the appropriateness of the scaffolds' microstructure to support cellular infiltration and proliferation, as well as the effect of elaborated ECM on scaffold mechanical behavior. However, it may be possible to utilize these scaffolds in a blood-contacting position without cell seeding [43]. This would be more attractive from a regulatory perspective and from a logistics perspective for "off-the-shelf" use. In this case, it would be hypothesized that native vascular or circulating cells would populate the scaffold and secrete ECM.

5. Conclusion

The function of any biomimetic heart valve replacement is dependent on adequate mechanical response to allow for a reasonable approximation of natural leaflet movement. For this goal, tissue engineered constructs must be extensible and mechanically anisotropic under planar loads [29] and possess sufficiently low flexural rigidity to allow for bending under physiologic pressures [31]. While electrospun polyurethanes have been suggested to be attractive for heart valve applications [17], no information on their flexural properties has been published. In this paper, methods for producing constructs with a customized bending modulus are presented. Modification of mandrel translational speed during fabrication was

shown to alter fiber intersection density, which was directly relatable to flexural response. Mixed fiber constructs with higher modulus were found to have higher bending and tensile moduli when secondary fibers were more stiff than PEUU, whereas sacrificial fibers within scaffolds were found to decrease overall construct moduli. Moreover, combining low translational speed during fabrication with sacrificial fiber populations produced constructs with both high mechanical anisotropy and low bending modulus.

Supplementary Material

Refer to Web version on PubMed Central for supplementary material.

Acknowledgments

Funding for this work was provided by NIH R01 HL-068816.

References

1. Bringman S, Conze J, Cuccurullo D, Deprest J, Junge K, Klosterhalfen B, et al. Hernia repair: the search for ideal meshes. Hernia. 2010; 14:81–7. [PubMed: 20012333]
2. Durst C, Cuchiara MP, Mansfield EG, West JL, Grande-Allen KJ. Flexural characterization of cell encapsulated pegda hydrogels with applications for tissue engineered heart valves. Acta Biomaterialia. 2011; 7:2467–76. [PubMed: 21329770]
3. Mirnajafi A, Raymer JM, McClure LR, Sacks MS. The flexural rigidity of the aortic valve leaflet in the commissural region. J Biomech. 2006; 39:2966–73. [PubMed: 16360160]
4. Gloeckner DC, Billiar KL, Sacks MS. Effects of mechanical fatigue on the bending properties of the porcine bioprosthetic heart valve. ASAIO J. 1999; 45:59–63. [PubMed: 9952009]
5. Dainese L, Guarino A, Burba I, Esposito G, Pompilio G, Polvani G, et al. Heart valve engineering: decellularized aortic homograft seeded with human cardiac stromal cells. Artif Cell Blood Sub. 2012; 21:125–34.
6. Cebotari S, Tudorache I, Jaekel T, Hilfiker A, Dorfman S, Ternes W, et al. Detergent decellularization of heart valves for tissue engineering: toxico-logical effects of residual detergents on human endothelial cells. Artif Organs. 2010; 34:206–10. [PubMed: 20447045]
7. Shinoka T. Tissue engineered heart valves: autologous cell seeding on biodegradable polymer scaffold. Artif Organs. 2002; 26:402–6. [PubMed: 12000435]
8. Hoerstrup SP, Kadner A, Melnitchouk S, Trojan A, Tracy J, Sodian R, et al. Tissue engineering of functional trileaflet heart valves from human marrow stromal cells. Circulation. 2002; 106:I143–50. [PubMed: 12354724]
9. Schmidt D, Mol A, Breymann C, Achermann J, Odermatt B, Gössi M, et al. Living autologous heart valves engineered from human prenatally harvested progenitors. Circulation. 2006; 114:I125–31. [PubMed: 16820561]
10. Stock U, Schenke-Layland K. Performance of decellularized xenogeneic tissue in heart valve replacement. Biomaterials. 2006; 27:1–2. [PubMed: 16026824]
11. Takagi K, Fukunaga S, Nishi A, Shojima T, Yoshikawa K, Hori H, et al. In vivo recellularization of plain decellularized xenografts with specific cell characterization in the systemic circulation: histological and immunohistochemical study. Artif Organs. 2006; 30:233–41. [PubMed: 16643381]
12. Cebotari S, Tudorache I, Ciubotaru A, Boethig D, Sarikouch S, Goerler A, et al. Use of fresh decellularized allografts for pulmonary valve replacement may reduce the reoperation rate in children and young adults: early report. Circulation. 2011; 124:S115–23. [PubMed: 21911800]
13. White J, Agnihotri A, Titus J, Torchiana D. A stentless trileaflet valve from a sheet of decellularized porcine small intestinal submucosa. Ann Thorac Surg. 2005; 80:704–7. [PubMed: 16039233]

14. Ruiz C, Iemura M, Medie S, Varga P, Van Alstine W, Mack S, et al. M K. Transcatheter placement of a low-profile biodegradable pulmonary valve made of small intestinal submucosa: a long-term study in a swine model. J Thorac Cardiov Surg. 2005; 130:477–84. [PubMed: 16077416]
15. Rippel RA, Ghanbari H, Seifalian AM. Tissue-engineered heart valve: future of cardiac surgery. World J Surg. 2012; 36:1581–91. [PubMed: 22395345]
16. Hashizume R, Fujimoto KL, Hong Y, Amoroso NJ, Tobita K, Miki T, et al. Morphological and mechanical characteristics of the reconstructed rat abdominal wall following use of a wet electrospun biodegradable polyurethane elastomer scaffold. Biomaterials. 2010; 31:3253–65. [PubMed: 20138661]
17. Courtney T, Sacks MS, Stankus J, Guan J, Wagner WR. Design and analysis of tissue engineering scaffolds that mimic soft tissue mechanical anisotropy. Biomaterials. 2006; 27:3631–8. [PubMed: 16545867]
18. Rutledge GC, Fridrikh SV. Formation of fibers by electrospinning. Adv Drug Deliver Rev. 2007; 59:1384–91.
19. Nisbet DR, Forsythe JS, Shen W, Finkelstein DI, Horne MK. A review of the cellular response on electrospun nanofibers for tissue engineering. J Biomater Appl. 2009; 24:7–29. [PubMed: 19074469]
20. Wright LD, Young RT, Andric T, Freeman JW. Fabrication and mechanical characterization of 3d electrospun scaffolds for tissue engineering. Biomed Mater. 2010; 5:055006. [PubMed: 20844321]
21. McCullen SD, Gittard SD, Miller PR, Pourdeyhimi B, Narayan RJ, Loboa EG. Laser ablation imparts controlled micro-scale pores in electrospun scaffolds for tissue engineering applications. Ann Biomed Eng. 2011; 39:3021–30. [PubMed: 21847685]
22. Neves NM, Campos R, Pedro A, Cunha J, Macedo F, Reis RL. Patterning of polymer nanofiber meshes by electrospinning for biomedical applications. Int J Nanomed. 2007; 2:433–48.
23. Guan J, Sacks MS, Beckman EJ, Wagner WR. Synthesis, characterization, and cytocompatibility of elastomeric, biodegradable poly(ester-urethane)ureas based on poly(caprolactone) and putrescine. J Biomed Mater Res. 2002; 61:493–503. [PubMed: 12115475]
24. Amoroso NJ, D'Amore A, Hong Y, Wagner WR, Sacks MS. Elastomeric electrospun polyurethane scaffolds: the interrelationship between fabrication conditions, fiber topology, and mechanical properties. Adv Mater. 2011; 23:1–6.
25. Agoram B, Barocas VH. Coupled macroscopic and microscopic scale modeling of fibrillar tissues and tissue equivalents. J Biomech Eng. 2001; 123:362–9. [PubMed: 11563762]
26. Sacks MS, Chuong CJ. Characterization of collagen fiber architecture in the canine central tendon. J Biomech Eng. 1992; 114:183–90. [PubMed: 1602761]
27. Bashur CA, Dahlgren LA, Goldstein AS. Effect of fiber diameter and orientation on fibroblast morphology and proliferation on electrospun poly(D, L-lactic-co-glycolic acid) meshes. Biomaterials. 2006; 27:5681–8. [PubMed: 16914196]
28. D'Amore A, Stella JA, Wagner WR, Sacks MS. Characterization of the complete fiber network topology of planar fibrous tissues and scaffolds. Biomaterials. 2010; 31:5345–54. [PubMed: 20398930]
29. Billiar KL, Sacks MS. Biaxial mechanical properties of the natural and glutaraldehyde treated aortic valve cusp – part i: experimental results. J Biomech Eng. 2000; 122:23–30. [PubMed: 10790826]
30. Merryman WD, Huang H-YS, Schoen FJ, Sacks MS. The effects of cellular contraction on aortic valve leaflet flexural stiffness. J Biomech. 2006; 39:88–96. [PubMed: 16271591]
31. Mirnajafi A, Raymer J, Scott MJ, Sacks MS. The effects of collagen fiber orientation on the flexural properties of pericardial heterograft biomaterials. Biomaterials. 2005; 26:795–804. [PubMed: 15350785]
32. Li W-J, Mauck RL, Cooper JA, Yuan X, Tuan RS. Engineering controllable anisotropy in electrospun biodegradable nanofibrous scaffolds for musculoskeletal tissue engineering. J Biomech. 2007; 40:1686–93. [PubMed: 17056048]
33. Nerurkar NL, Elliott DM, Mauck RL. Mechanics of oriented electrospun nanofibrous scaffolds for annulus fibrosus tissue engineering. J Orthopaed Res. 2007; 25:1018–28.

34. Wang C-Y, Zhang K-H, Fan C-Y, Mo X-M, Ruan H-J, Li F-F. Aligned natural-synthetic polyblend nanofibers for peripheral nerve regeneration. Acta Biomaterialia. 2011; 7:634–43. [PubMed: 20849984]

35. Kai D, Prabhakaran MP, Jin G, Ramakrishna S. Guided orientation of cardiomyocytes on electrospun aligned nanofibers for cardiac tissue engineering. J Biomed Mater Res. 2011; 98B: 379–86.

36. Lowery JL, Datta N, Rutledge GC. Effect of fiber diameter, pore size and seeding method on growth of human dermal fibroblasts in electrospun poly(epsilon-caprolactone) fibrous mats. Biomaterials. 2010; 31:491–504. [PubMed: 19822363]

37. Shi Q, Wan K-T, Wong S-C, Chen P, Blackledge TA. Do electrospun polymer fibers stick? Langmuir. 2010; 26:14188–93. [PubMed: 20681738]

38. Laws V. On the mixture rule for strength of fibre reinforced cements. J Mater Sci Lett. 1983; 2:527–31.

39. Roy R, Kohles SS, Zaporojan V, Peretti GM, Randolph MA, Xu J, et al. Analysis of bending behavior of native and engineered auricular and costal cartilage. J Biomed Mater Res. 2004; 68:597–602.

40. Westreich RW, Courtland HW, Nasser P, Jepsen K, Lawson W. Defining nasal cartilage elasticity: biomechanical testing of the tripod theory based on a cantilevered model. Arch Facial Plast Surg. 2007; 9:264–70. [PubMed: 17638761]

41. Baker BM, Gee AO, Metter RB, Nathan AS, Marklein Ra, Burdick JA, Mauck RL. The potential to improve cell infiltration in composite fiber-aligned electrospun scaffolds by the selective removal of sacrificial fibers. Biomaterials. 2008; 29:2348–58. [PubMed: 18313138]

42. Patel AS, Smith A, Attia RQ, Mattock K, Humphries J, Lyons O, et al. Encapsulation of angiogenic monocytes using bio-spraying technology. Integr Biol. 2012; 4:628–32.

43. Williams SK, Kleinert LB, Patula-Steinbrenner V. Accelerated neovascularization and endothelialization of vascular grafts promoted by covalently bound laminin type 1. J Biomed Mater Res A. 2011; 99:67–73. [PubMed: 21800416]

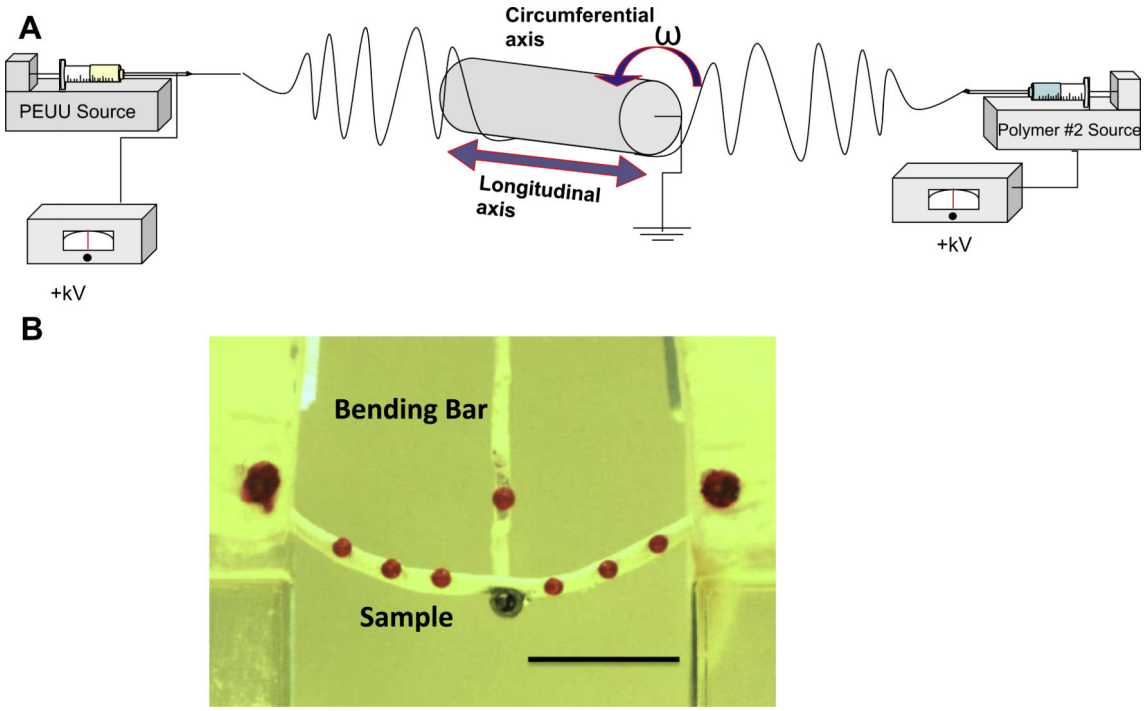

Fig. 1.

(A) Schematic of electrospinning apparatus for two-component scaffolds. PEUU was fed from the same location for every group. The mandrel was rotated and translated along its longitudinal axis at varying speeds. Secondary polymer fibers were introduced through separate nozzles. (B) Image of a polymeric specimen loaded in the bending device (scale bar = 1 cm).

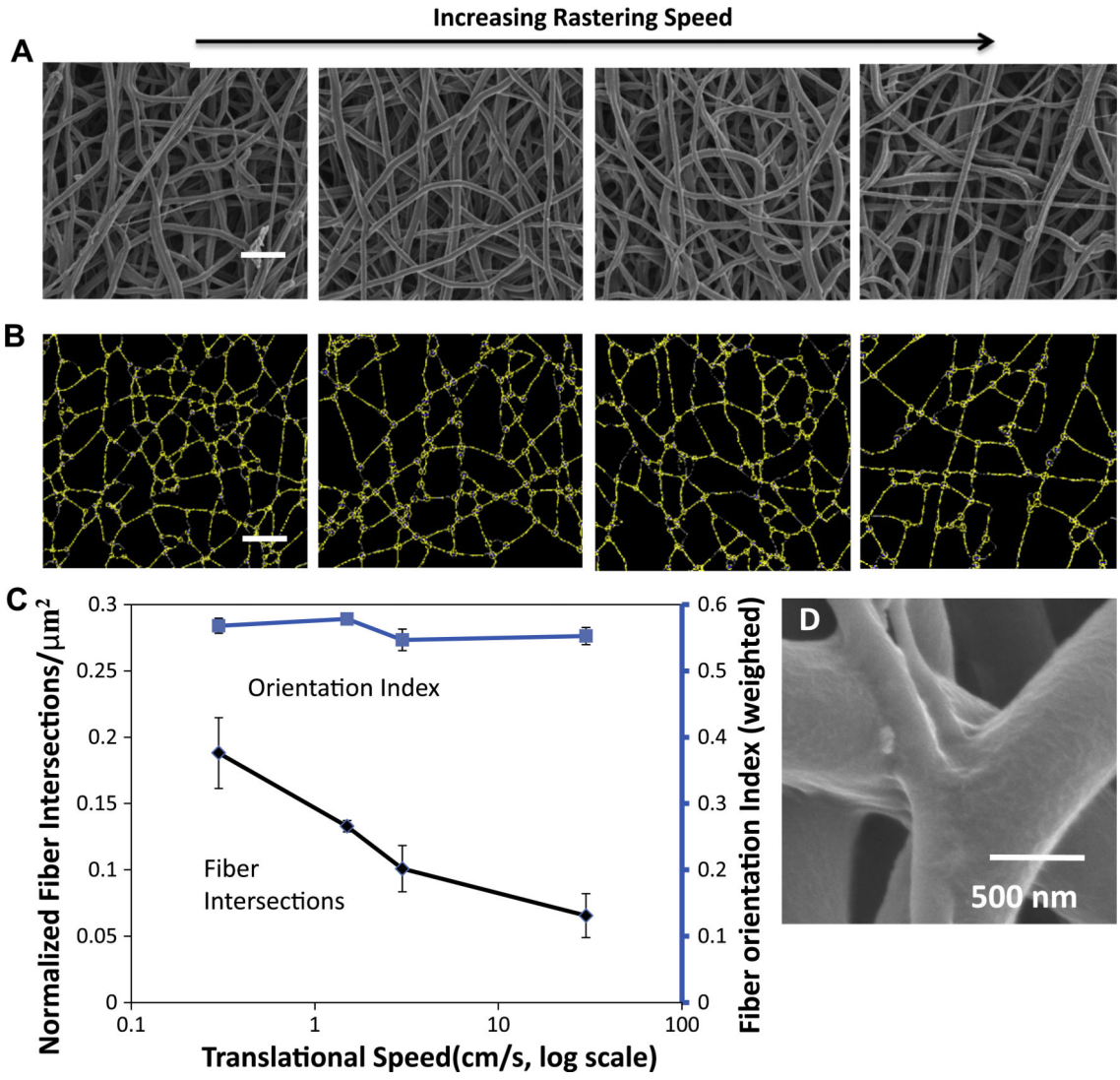

Fig. 2.

(A) SEM micrographs of representative scaffolds from each translated group (scale bar = 5 μm) and (B) their corresponding digitized structure. (C) A plot depicting the quantitative relationship between translational speed during fabrication and microstructural elements. (D) High magnification morphology of a fiber intersection.

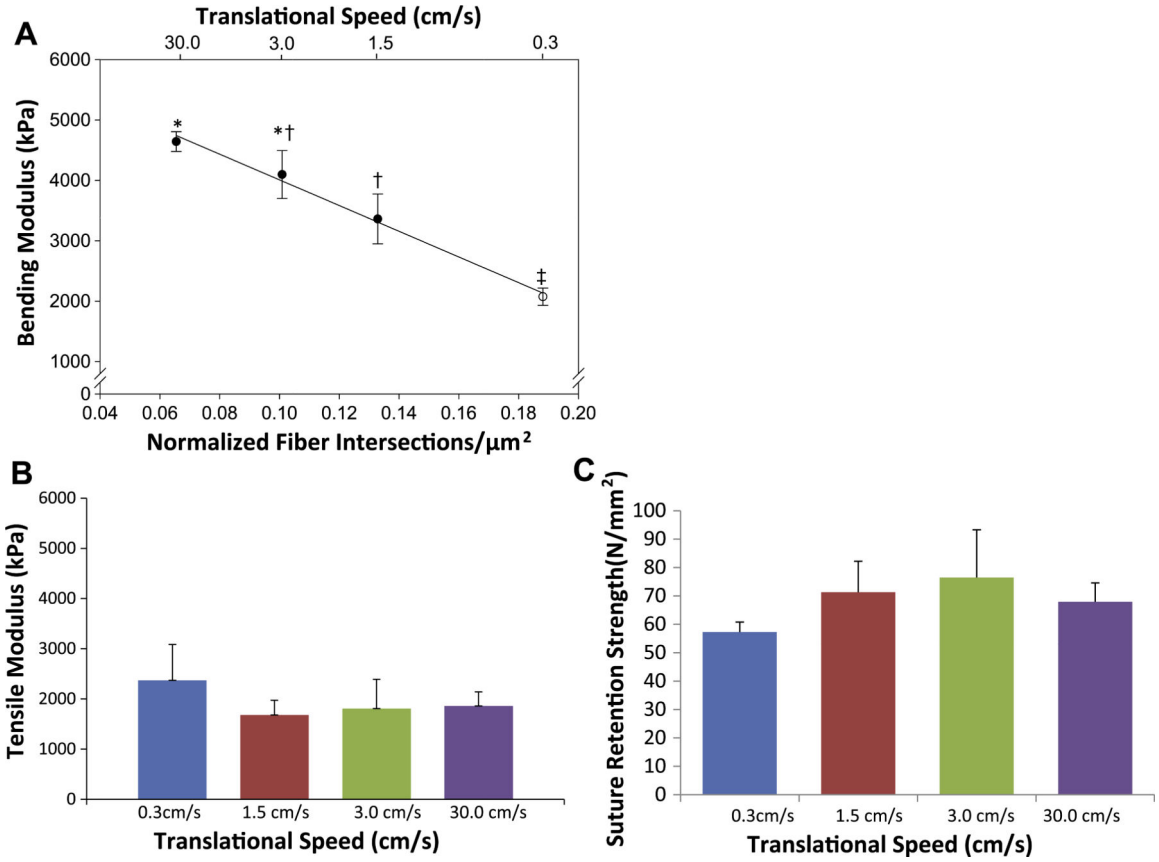

Fig. 3.

(A) The relationship between translational velocity during fabrication (top *x* axis), fiber intersection density (bottom *x* axis), and bending modulus (*y* axis). (B) Uniaxial tensile modulus of electrospun scaffolds fabricated under different translational velocities. (C) Suture retention strengths of scaffolds fabricated under different translational velocities.

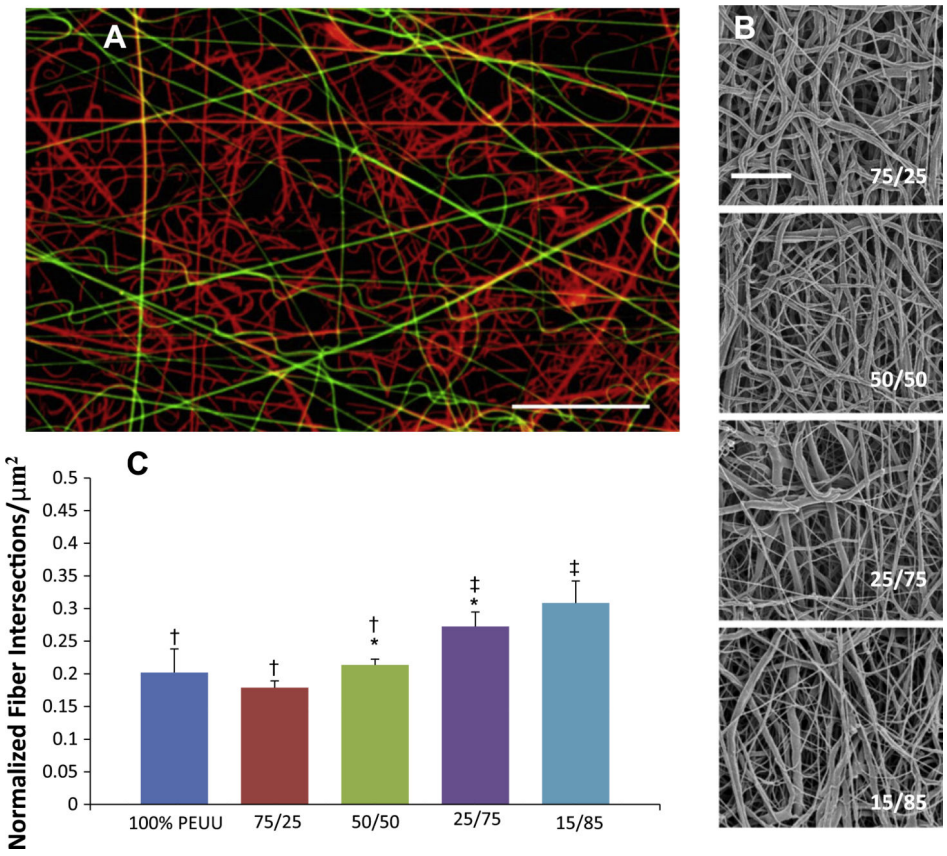

Fig. 4.

(A) Fluorescent micrograph qualitatively depicting relative distribution of PEUU fibers (green) to PCL fibers (red) in a 75/25 volume flow rate ratio construct. Scale bar = 20 μm. (B) Microstructure of representative PEUU/PCL blended scaffolds. Scale bar = 10 μm. (C) Change in fiber intersection density observed between PEUU/PCL ratios. No other differences in microstructural features were observed.

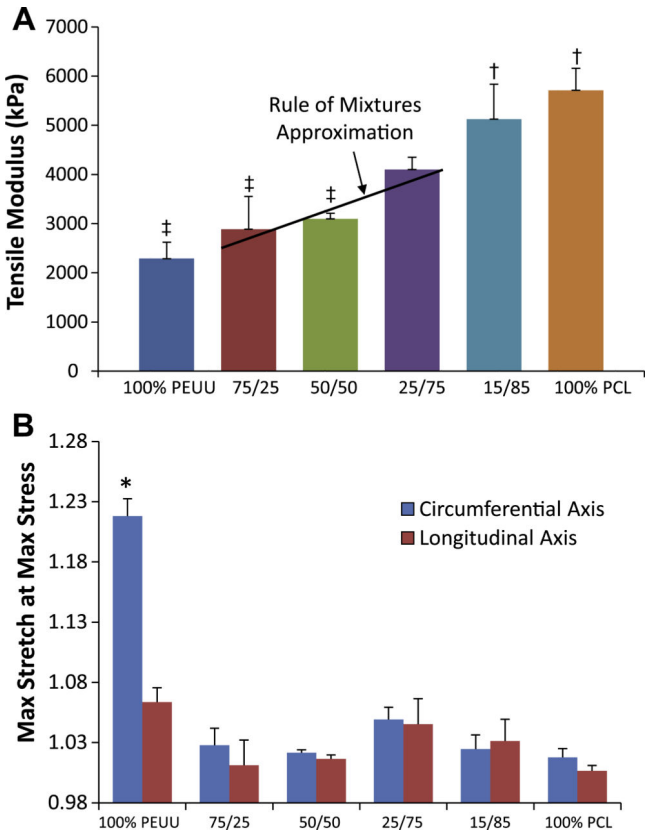

Fig. 5.

(A) Uniaxial tensile mechanical response of constructs containing increasing quantities of PCL fibers. (B) Planar biaxial mechanical properties of PEUU:PCL blended scaffolds groups with different symbols (‡,†,*) are significantly different from one another ($p < 0.05$).

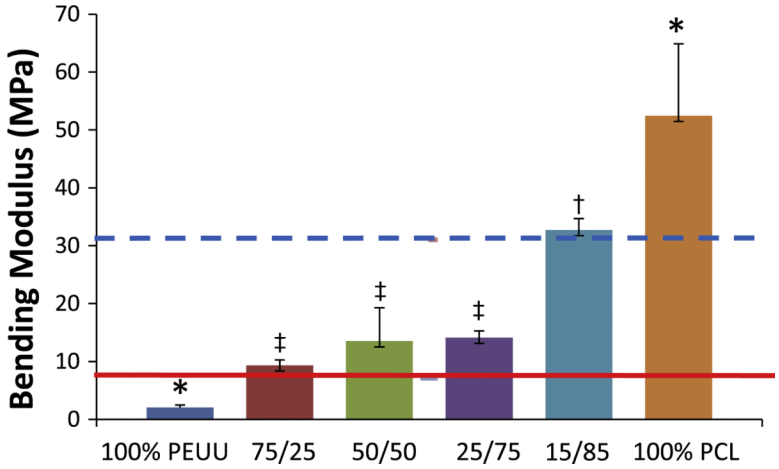

Fig. 6.

Bending modulus of mixed polymer constructs at varying ratios of PEUU:PCL. Groups with different symbols (‡,†) are significantly different from one another, and groups with (*) are significantly different from all other groups ($p < 0.05$). Solid reference line indicates the bending modulus of native costal cartilage [39]. Dashed reference line indicates the bending modulus of the intact septum [40].

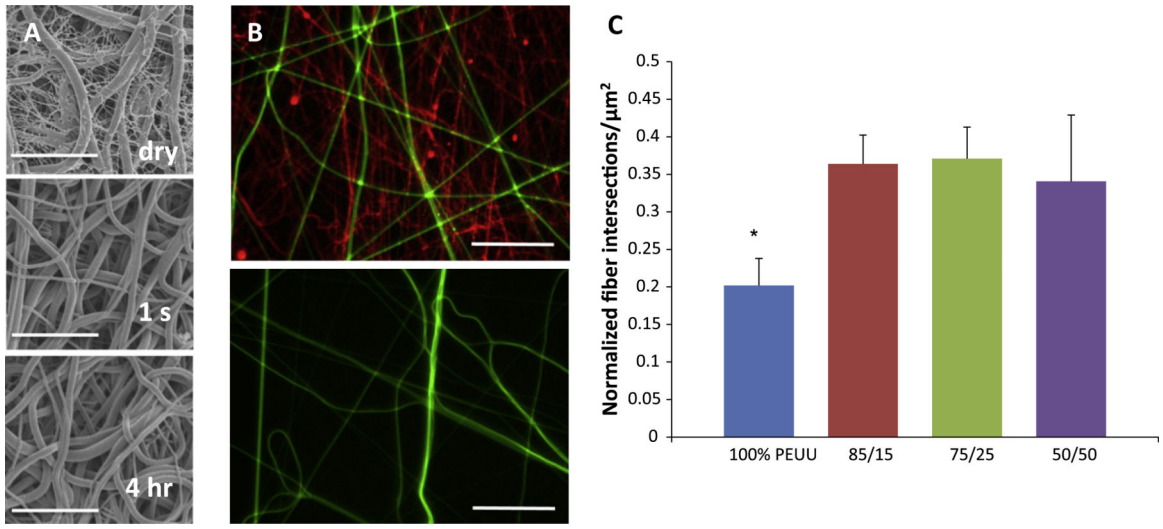

Fig. 7.

(A) Representative structural images of PEUU/PEO 75/25 scaffolds as-spun (dry), after 1 s and after 4 h of soaking in water. Scale bar = 10 μm. (B) Fluorescent micrographs of PEUU (green)/PEO (red) blended constructs before (above) and after (below) treatment with water. Scale bar = 20 μm. (C) Difference in normalized fiber intersection density between as-spun 100% PEUU constructs and constructs following removal of PEO fibers; *indicates statistical significance ($p < 0.05$).

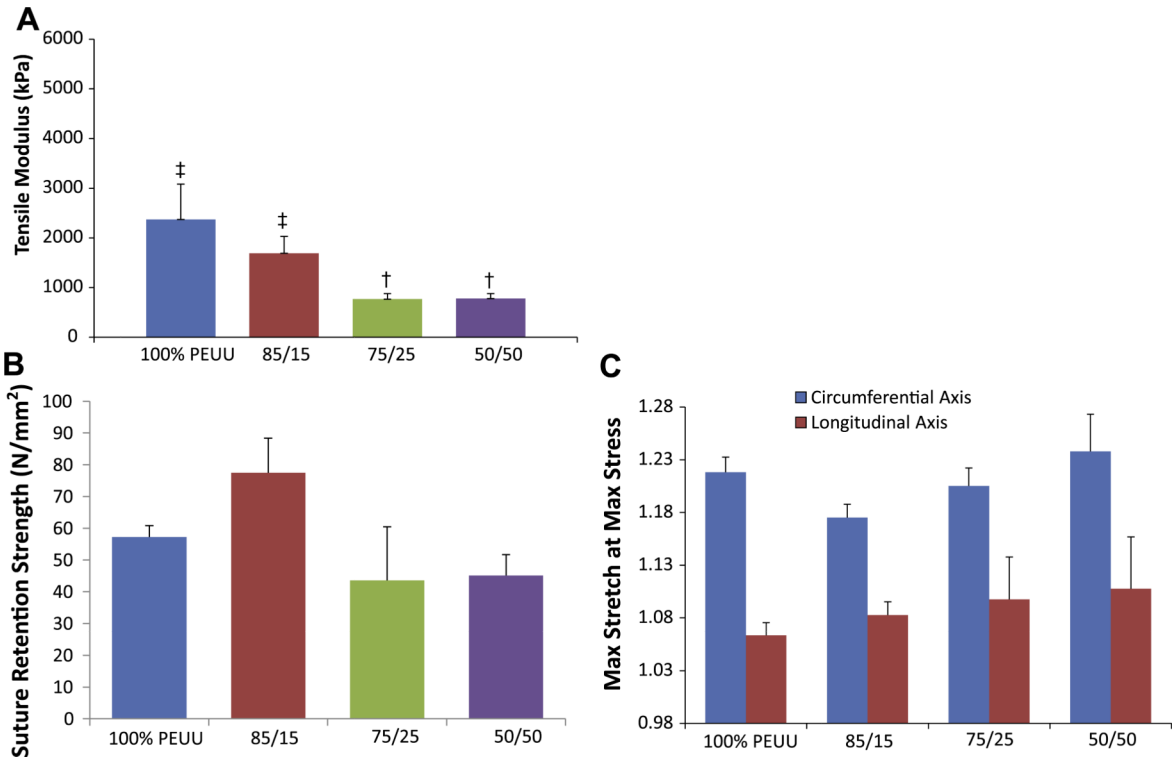

Fig. 8.

(A) Tensile modulus of constructs containing varying quantities of PEO following contact with water. (B) Suture retention strength of constructs following PEO fiber removal. (C) Biaxial mechanical response of constructs following PEO fiber removal. Groups with different symbols (‡,†) are significantly different from one another ($p < 0.05$).

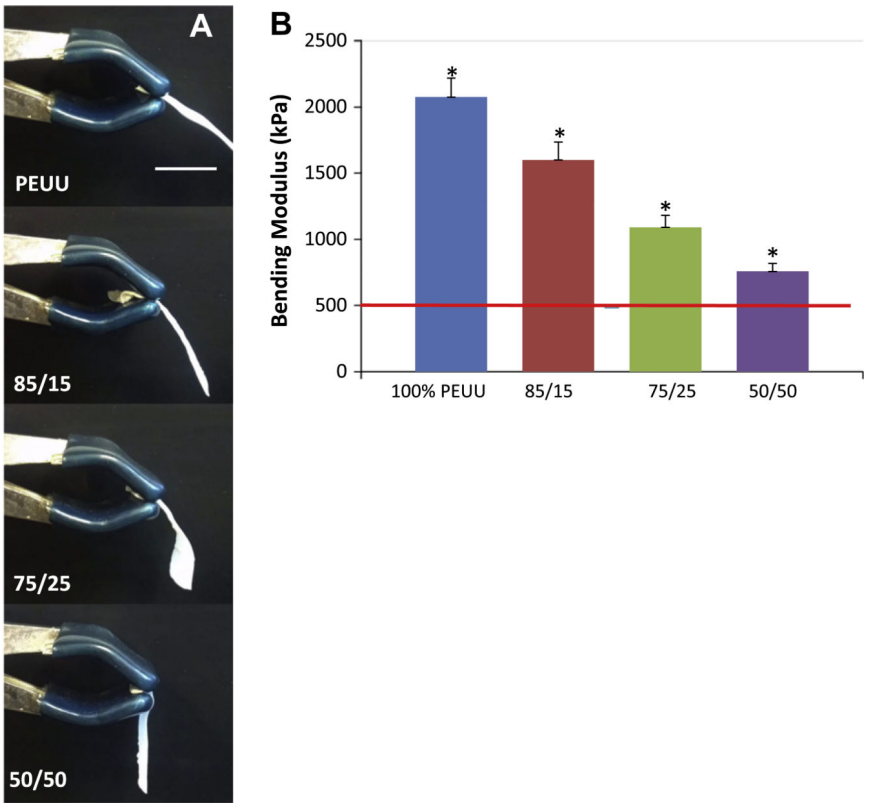

Fig. 9.

(A) Qualitative depiction of constructs originally containing varying amounts of PEO placed in a cantilever position following contact with water. (B) Bending modulus of constructs following PEO fiber removal. Reference line indicates the bending modulus of the native pulmonary valve (491 kPa) [30]. *indicates statistical significance ($p < 0.05$).